Noise and Large-Signal Characterization of a Thin-Film MHEMT Feedback Amplifier in Multilayer MCM-D Technology

R. Vandersmissen, D. Schreurs, G. Dambrine*, G. Carchon, and G. Borghs

IMEC, MCP, Kapeldreef 75, B-3001 Leuven, BELGIUM
*IEMN, UMR CNRS, 59655 Villeneuve D'Ascq, Cedex, FRANCE
Phone: +32-16-288056, e-mail: raf.vandersmissen@imec.be

Keywords: MHEMT, Large-Signal, Microwave Noise, Feedback Amplifier, MCM-D

Abstract

In this paper, we investigate the noise and large-signal behavior of a feedback amplifier in multilayer thin-film MCM-D technology. A small-signal equivalent model (including noise) of the active devive, a thin-film MHEMT, is identified. A large-signal state-space transistor model is built from time-domain data. These models are implemented in a circuit simulator and can accurately predict the noise and large-signal behavior of the feedback amplifier.

INTRODUCTION

MCM-D technology has proven to be a viable candidate for the integration and interconnection of high-quality microwave and RF applications [1, 2]. Recently, we have shown that thin-film Ge-based metamorphic HEMTs (MHEMTs) can be used in MCM-D circuits [3, 4]. After substrate removal, the MHEMTs (thickness < 3 µm), are embedded in the bottom BCB layer of the MCM-D layer structure. This technique leads to a reduction in interconnection length (between transistor and passive devices), size and weight. Figure 1 shows a schematic cross-section of this combination of III-V and MCM-D technology.

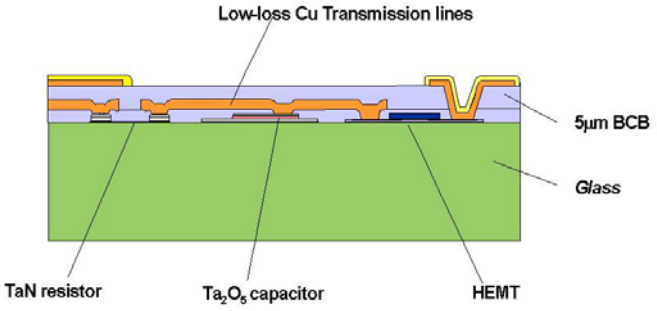

Figure 1: Schematic cross-section of integrated passives and embedded Ge-based HEMT in MCM-D technology.

In this work, we investigate the accuracy of a small-signal transistor model (including noise) and a large-signal transistor model for a thin-film MHEMT. The noise figure and large-signal behavior of the amplifier can be predicted accurately.

TRANSISTOR MODELING

The small-signal equivalent transistor model (including noise) is extracted using S-parameter measurements. The noise parameters are determined using the F_{50} method [5]. The noise parameters can be directly obtained from the frequency variation of the noise figure F_{50} corresponding to a 50 Ω generator impedance. This method has the following advantages:

- no need for an automatic input tuner;
- well suited for measurements in the mm-wave range.

The NF_{min} (minimum noise figure) of a thin-film MHEMT is higher than the NF_{min} of a comparable GaAs MHEMT due a higher channel temperature in the thin devices (see figure 2).

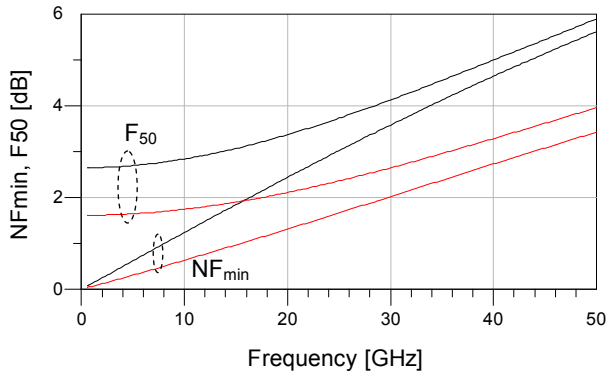

Figure 2: Minimum noise factor (F_{min}) and noise factor with 50 Ω source (F_{50}) of GaAs MHEMT (red) and thin-film MHEMT (black).

A large-signal state-space model is built from time-domain data, obtained by performing large-signal vector measurements using a Large-Signal Network Analyzer (LSNA) [6, 7]. The basic principle of the modeling method

involves that the considered two-port devices can be described by equations of the form:

$$i_1(t) = f_1\left(v_1(t), v_2(t), \dot{v}_1(t), \dot{v}_2(t), \ddot{v}_1(t), \cdots, \dot{i}_1(t), \dot{i}_2(t)\right)$$
$$i_2(t) = f_2\left(v_1(t), v_2(t), \dot{v}_1(t), \dot{v}_2(t), \ddot{v}_1(t), \cdots, \dot{i}_1(t), \dot{i}_2(t)\right)$$

with $i_1(t)$ and $i_2(t)$ the terminal currents, $v_1(t)$ and $v_2(t)$ the terminal voltages, and the superscript dots representing the (higher order) time derivatives. The objective of the modeling technique is to find the number of independent or state variables, and consequently to determine the functional relationships $f_1(.)$ and $f_2(.)$ by fitting the measured terminal currents to the measured state variables. Artificial Neural Networks (ANNs) are used to describe f_1 and f_2 [8].

At the start of the modeling process, operating bounds for the model are established by predefining the minimum and maximum instantaneous target values of the terminal voltages v_1 and v_2. These bounds define the v_1-v_2 operating region within the state space for which the model is to be developed and used. To enable accurate identification of the device dynamics, the measured time-domain data need to sample this operating region efficiently. For the considered thin-film MHEMTs, we have fixed the fundamental frequency to 1 GHz and performed measurements at various input powers (ranging from –23 dBm to –1 dBm) and DC bias conditions (V_{gs} ranging from –0.55 V to –0.3 V, V_{ds} ranging from 0.7 V to 1 V).

The next step is to determine the independent (or state) variables. One can deduce from the known physics of a HEMT, that the dominant independent variables are the terminal voltages, as well as the corresponding first and second order time derivatives.

Consequently, the functional relationships $f_1(.)$ and $f_2(.)$ have to be determined by fitting the measured time-domain terminal currents towards the measured independent variables. For that purpose, we prefer to ANNs. For this particular case, we use an artificial neural network with six inputs (the voltages up to the second derivative). The ANN is trained using the back-propagation algorithm, as implemented in the NeuroModeler program, which is described in detail in [9]. We have found that an ANN with a single hidden layer of 24 neurons provides the best trade-off between model accuracy and model complexity.

Figures 3 and 4 show a comparison between the measured and simulated time-domain waveforms of the transistor terminal currents. The average training error of the ANN is 0.5%.

The state-space model can be implemented in ADS by means of a Symbolically Defined Device (SDD). The SDD can calculate the time-derivatives of the terminal voltages at each time step in the simulation, as well as the dissipated power if required, enabling the fitting functions for the currents to be evaluated. The accuracy of this model on circuit level will be evaluated in the next section.

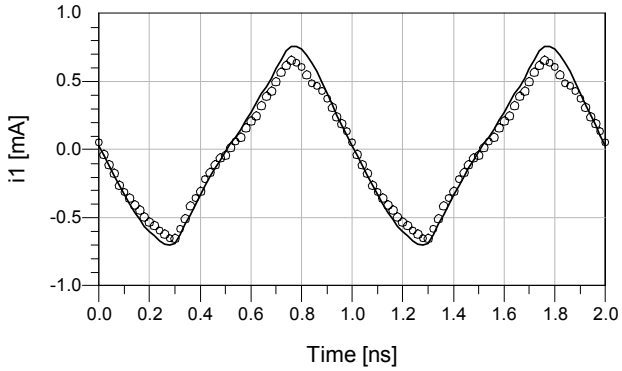

Figure 3: Measured (o) and simulated (solid line) time-domain waveforms (1 GHz) of the gate current (i_1). The DC bias conditions are: V_{ds} = 0.7 V, V_{gs} = -0.3 V. The input power is –5 dBm.

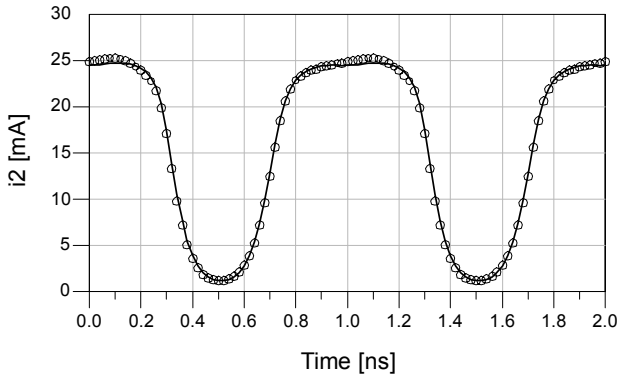

Figure 4: Measured (o) and simulated (solid line) time-domain waveforms (1 GHz) of the drain-source current (i_2). The DC bias conditions are: V_{ds} = 0.7 V, V_{gs} = -0.3 V. The input power is –5 dBm.

AMPLIFIER MEASUREMENT RESULTS

Figure 5 shows a picture of the MHEMT-based feedback amplifier in MCM-D technology. The gate length of the MHEMT is 200 nm, the gate width is 2 × 50 μm. The embedded active device (dashed line) and the frequency-dependent feedback loop are clearly visible. Due to the relatively low total g_m value (70 mS) of the active device, the amplifier gain will be rather low. The low g_m also makes it difficult to take the value of the feedback resistance close to the value for a good input or output match as for such low resistance value, the gain would drop to almost unity. Instead a relatively high feedback resistance value (310 Ω) has been taken at the expense of a higher reflection. Note that neither input nor output matching networks are included in the circuit.

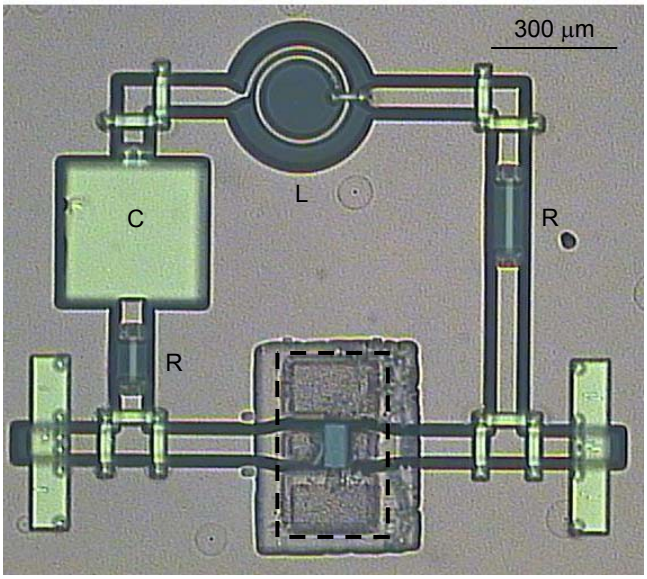

Figure 5: Picture of the MCM-D feedback amplifier (CPW lay-out) with embedded MHEMT.

Figure 6 shows the gain and in- and output reflection of the amplifier. A very flat gain of 9 dB (± 0.5 dB) over a frequency band from 1 to 13 GHz and a very good match between simulation (using the small-signal model) and measurement have been achieved.

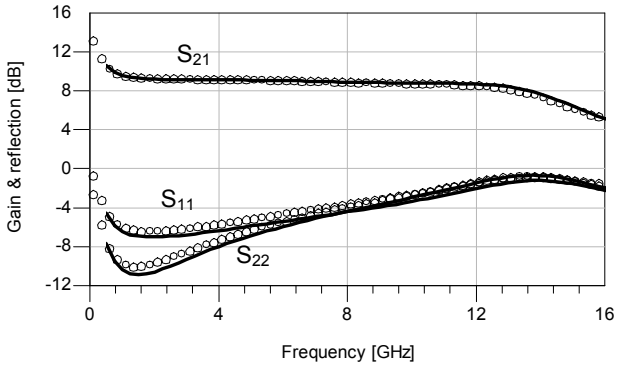

Figure 6: Measured (o) and simulated (solid line) gain (S_{21}), input reflection (S_{11}) and output reflection (S_{22}) of the feedback amplifier. The DC bias conditions are: V_{ds} = 1 V, V_{gs} = -0.4 V.

Figure 7 shows the noise figure (NF) of the feedback amplifier from 6 to 13 GHz. Note that this particular feedback amplifier has not been optimized for low noise. A good match between simulation and measurement is shown.

In figures 8 and 9, the measured and simulated time-domain waveforms of the input and output current of the amplifier (for three different input powers) are compared.

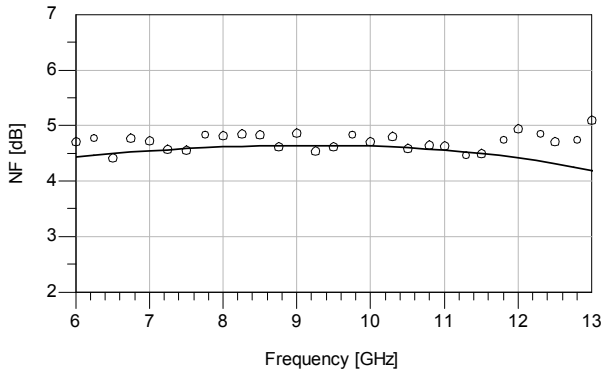

Figure 7: Measured (o) and simulated (solid line) noise figure (NF) of the feedback amplifier. The DC bias conditions are: V_{ds} = 1 V, V_{gs} = -0.4 V.

Based on these plots, we can conclude that a good model prediction can be obtained, providing the range of measurements used in the training process span all instantaneous conditions of the verification measurements.

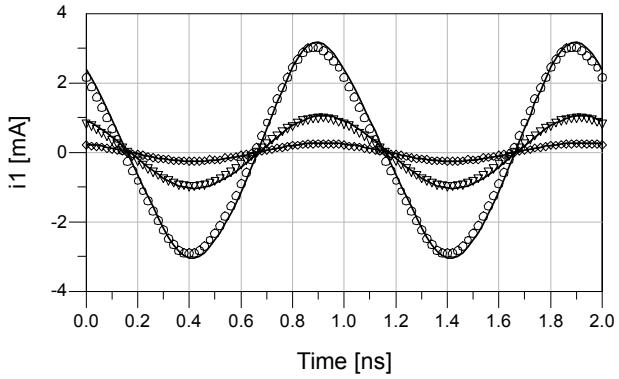

Figure 8: Measured (◊: -23 dBm input power, ∇: -11 dBm input power, o: -1 dBm input power) and simulated (solid line) time-domain waveforms of the input current (i1). The DC bias conditions are: V_{ds} = 1 V, V_{gs} = -0.4 V.

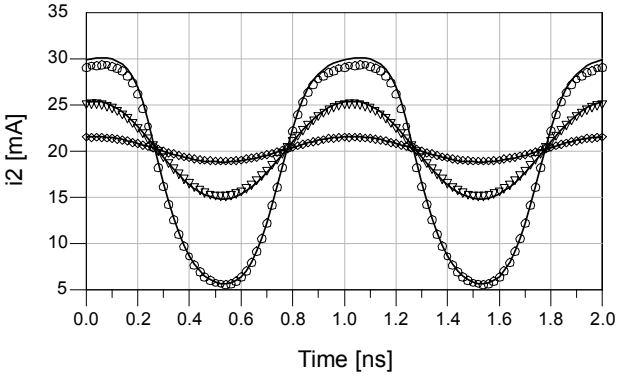

Figure 9: Measured (◊: -23 dBm input power, ∇: -11 dBm input power, o: -1 dBm input power) and simulated (solid line) time-domain waveforms of the output current (i2). The DC bias conditions are: V_{ds} = 1 V, V_{gs} = -0.4 V.

The visual interpretation of the model accuracy can also be quantified objectively by the use of metrics. Table 1 lists the metric values for the scattered waves b_1 (at the input of the amplifier) and b_2 (at the output of the amplifier). We consider a weighted metric in the frequency domain [10].

$$S(x,\hat{x}) = \left|x_0 - \hat{x}_0\right| + \sum_{i=1}^{N} \frac{\left|x_i\right|}{\sum_{j=1}^{N}\left|x_j\right|}\left|x_i - \hat{x}_i\right|$$

The value S summarizes the differences between modeled ($\hat{x}$) and measured (x) quantities, where i and j are harmonic indices, N is the number of harmonics considered, and the subscript 0 denotes the DC value. By using this formalism, errors in predicting the dominant harmonics have a relatively larger contribution to the overall metric value. From table 1, it can be noted that the accuracy in predicting b_1, is slightly better compared to that of b_2. The reason is that the device nonlinearities are more dominant at the port two side.

Table 1: Weighted metric to quantify the accuracy of the large-signal state-space model in the feedback amplifier.

	b_1	b_2
Weighted metric [V]	$4.80 \cdot 10^{-3}$	$1.54 \cdot 10^{-2}$

CONCLUSIONS

In this paper, the microwave noise and large-signal behavior of a feedback amplifier, based on an embedded metamorphic HEMT, in MCM-D technology have been investigated. A small-signal equivalent MHEMT model (including noise) and a large-signal state-space MHEMT model can accurately predict the noise figure and large-signal behavior of the feedback amplifier.

ACKNOWLEDGEMENTS

The authors would like to thank E. Vandenplas, S. De Jonge and J. Hendrickx for processing work. Furthermore, financial support from IWT and FWO was appreciated.

REFERENCES

[1] R. G. Arnold, et al., "Silicon MCM-D technology for RF integration," Proceedings of the 6th International Conference and Exhibition on Multichip Modules, pp. 340-344, 1997.

[2] R. C. Frye, et al., "Silicon MCM-D with integrated passive components for RF wireless applications," Proceedings of the IEEE MCM Conference, pp. 33-37, 1997.

[3] R. Vandersmissen, et al., "Feedback amplifier based on an embedded HEMT in thin-film multilayer MCM-D technology," Proceedings of the European GaAs and related III-V compounds Applications Symposium (GAAS), pp. 423-426, 2003.

[4] R. Vandersmissen, et al., "Integrated circuits using embedded III-V-on-Ge MHEMTs in multilayer thin-film technology," Digest of papers of International Conference on GaAs Manufacturing Technology (GaAsMANTECH), pp. 87-90, 2003.

[5] G. Dambrine, et al., "A new method for on-wafer noise measurement," IEEE Trans. Microwave Theory Tech., Vol. 41, No. 3, 1993.

[6] D. Schreurs, et al., "Efficient construction of a large-signal behavioral HEMT model from automated vectorial large-signal measurements," IEEE Proceedings of International Symposium on Electron Devices for Microwave and Optoelectronic Applications (EDMO), pp. 217-221, 2001.

[7] J. Verspecht, et al., "Accurate on wafer measurement of phase and amplitude of the spectral components of incident and scattered voltage waves at the signal ports of a nonlinear microwave device," IEEE Digest of International Microwave Symp. (MTT-S), pp. 1029-1032, 1995.

[8] D. Schreurs, et al., "Artificial neural network model for HEMTs constructed from large-signal time-domain measurements," 59th ARFTG Conference Digest, pp. 31-36, 2002.

[9] Q. J. Zhang and K. C. Gupta, "Neural networks for RF and microwave design," Artech House, 2000.

[10] K. Remley, et al., "Repeat measurements and metrics for nonlinear model development," IEEE MTT-S International Microwave Symposium Digest, pp. 2169-2172, 2002.

ACRONYMS

HEMT: High Electron Mobility Transistor
MHEMT: Metamorphic HEMT
MCM-D: Multichip Module-Deposition
LSNA: Large-Signal Network Analyzer
SDD: Symbolically Defined Device